ChemComm

COMMUNICATION

View Article Online
View Journal | View Issue

Cite this: *Chem. Commun.*, 2016, 52, 1971

Received 14th November 2015,
Accepted 9th December 2015

DOI: 10.1039/c5cc09432a

www.rsc.org/chemcomm

An effective strategy to boost the robustness of metal–organic frameworks *via* introduction of size-matching ligand braces†

Xiuli Wang,‡*[ab] Wen-Yang Gao,‡[b] Jian Luan,[a] Lukasz Wojtas[b] and Shengqian Ma*[b]

Framework fragility upon the removal of guest solvent molecules has remained an issue for a substantial amount of metal–organic frameworks (MOFs). To address this issue, in this work we illustrate a strategy for the introduction of size-matching ligands as braces that are deliberately anchored onto the open metal sites to support and segment the pores thereby boosting the framework robustness. This is exemplified by employing 4,4′-bipyridine as a brace to bridge two trigonal prismatic clusters of $Co_3(\mu_3\text{-}O)(COO)_6$, generating a robust MOF that exhibits permanent porosity and selective gas adsorption behaviors.

Over the past two decades, metal–organic frameworks (MOFs)[1] have been attracting extensive research interest due to their controllable pore size (surface area) and versatile structural topologies.[2] These intriguing structural features enable MOFs to be a potential platform for a variety of applications in gas storage and separation,[3] heterogeneous catalysis,[4] sensing[5] and other areas.[6] Composed of multidentate organic ligands and metal ions or *in situ* formed secondary building units (SBUs), MOFs usually exhibit large open accessible channels or cages, which can be utilized to accommodate guest molecules from gas storage/separation, catalytic substrate, sensing and drug delivery.[7] However, all these applications largely rely on the premise that MOFs possess permanent porosity. Albeit there have emerged numerous permanently porous MOFs over the past decade, a substantial amount of MOFs still experience framework collapse upon removal of solvent molecules, which inevitably undermines their potential for the aforementioned applications.[8] To address this issue, several strategies have been developed to boost the robustness of MOFs or strengthen the open framework structures by virtue of multiple strong coordination bonding,[9] interpenetration,[10] variation of functional groups,[11] and surface modification.[12] In this contribution, we demonstrate an alternative strategy as a proof-of-concept to stabilize MOFs *via* introduction of size-matching ligands as braces that are deliberately anchored onto the open metal sites to support the pores, as shown in Scheme 1. Moreover, the inserted ligand[13] braces are able to segment large channels into small domains, which may render molecular sieving effect or promote gas separation capability *via* increase of host–guest interactive sites.

To illustrate our strategy, we selected a nanotubular MOF (**1**), $[Co_3(\mu_3\text{-}O)(adc)_3(DMA)_3]\cdot 2(C_2H_6NH_2)$ (H_2adc = 9,10-anthracenedicarboxylic acid, DMA = *N*,*N*′-dimethylacetamide), for proof of principle. We employed 4,4′-bipyridine (4,4′-bpy) as the brace to bridge two trigonal prismatic clusters of $Co_3(\mu_3\text{-}O)(COO)_6$, affording a robust MOF (**2**), $[Co_3(\mu_3\text{-}O)(adc)_3(4,4'\text{-}bpy)(DMA)]\cdot 2(C_2H_6NH_2)$. The stabilized framework **2** is permanently microporous and exhibits a molecular sieving effect with a selective adsorption of CO_2 and O_2 over N_2.

Solvothermal reactions of $Co(NO_3)_2\cdot 6H_2O$ and H_2adc in the solvent of DMA gave rise to orange crystals of complex **1** and red crystals of complex **2** in the presence of 4,4′-bpy, respectively. Single-crystal X-ray crystallographic analysis revealed that complex **1** crystallized in the trigonal space group

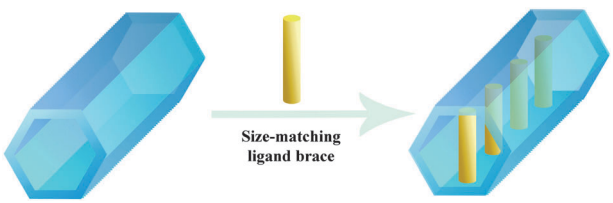

Scheme 1 Schematic representation of the strategy to boost the robustness of MOFs *via* introduction of size-matching ligand braces into the open channels.

[a] *Department of Chemistry, Bohai University, Jinzhou, 121000, P. R. China. E-mail: wangxiuli@bhu.edu.cn; Fax: +86-416-3400158; Tel: +86-416-3400158*
[b] *Department of Chemistry, University of South Florida, 4202 E. Fowler Avenue, Tampa, Florida 33620, USA. E-mail: sqma@usf.edu; Fax: +1-813-974-3203; Tel: +1-813-974-5217*

† Electronic supplementary information (ESI) available: Experimental procedures for the synthesis of complexes **1** and **2**, PXRD, TGA, IR and structure pictures of complexes **1** and **2**. CCDC 1436005 and 1435998. For ESI and crystallographic data in CIF or other electronic format see DOI: 10.1039/c5cc09432a

‡ Equal contribution.

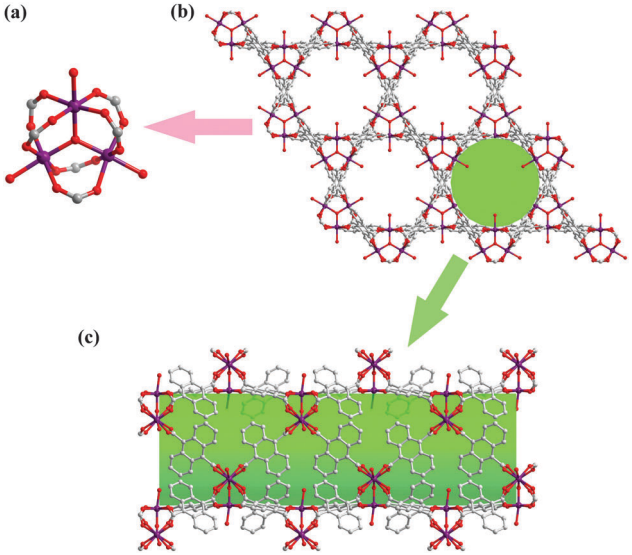

Fig. 1 (a) The cobalt trigonal prismatic SBU; (b) the view of the packing framework of complex **1**; (c) the side view of the hexagonal nanotubular channel in complex **1**.

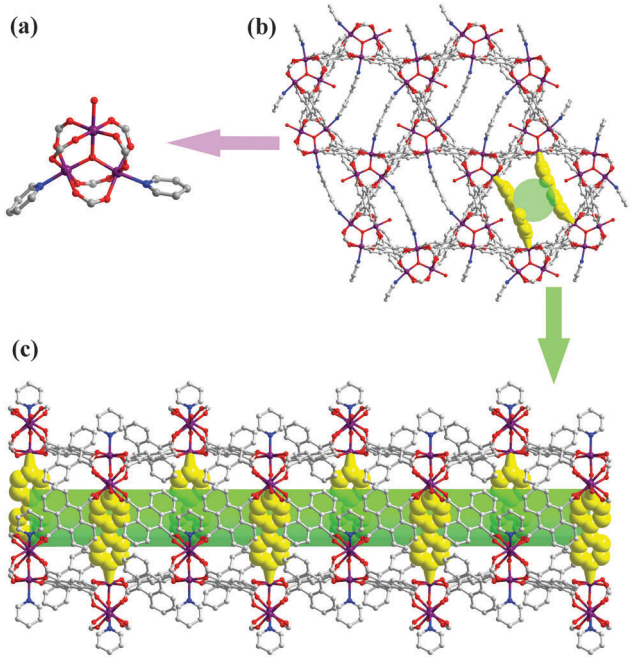

Fig. 2 (a) The cobalt trigonal prismatic SBU of complex **2** (the indicated pyridine units are from 4,4′-bpy molecules); (b) the view of the packing framework of complex **2** (part of the inserted 4,4′-bpy molecules highlighted with yellow color); and (c) the side view of the nanotubular channel.

of $P\bar{3}_1c$,§ which is built on cobalt trigonal prismatic SBUs of $[Co_3(\mu_3\text{-}O)(COO)_6]$ (Fig. 1a) and adc ligands. Accordingly, complex **1** is isostructural with the nickel-based PCN-19.[14] In the trigonal prismatic SBU, three Co ions and the μ_3-O atom are on the same plane. Each Co ion adopts the octahedral coordination geometry, which is six-coordinated by a μ_3-O atom, four carboxyl O atoms from four adc ligands and an oxygen atom from the terminal solvent molecule. Two adjacent Co ions are bridged by two carboxyl groups from two different adc ligands, forming a tricobalt SBU. Each tricobalt SBU connects with six adc ligands, and each adc ligand links two tricobalt SBUs to generate honeycomb-like hexagonal channels along the *c*-axis direction, as illustrated in Fig. 1b and c. Calculated using PLATON,[15] complex **1** has a solvent accessible volume of 52.6% after the removal of the coordinated solvent molecules. From a topological viewpoint, the overall structure of complex **1** is a semiregular, non-uniform $(4^9\cdot6^6)$-Archimedean (acs) net (Fig. S1, ESI†).

Complex **2** crystallizes in the monoclinic space group of $P2_1/n$,§ constructed by cobalt trigonal prismatic SBUs (Fig. 2a) and adc ligands, and 4,4′-bpy ligands. Complex **2** adopts a similar cobalt trigonal prismatic cluster to that of complex **1**, except two pyridine units from two 4,4′-bpy replacing two coordinated solvent molecules (Fig. 2a). This leads the tricobalt SBU to an eight-connected node instead of six-connected node in **1**. As shown in Fig. 2b and c, each 4,4′-bpy bridges two meta-tricobalt SBUs in the hexagonal nanotubular channel, which can be regarded as the brace supporting the open channels. As can be seen, the molecule of 4,4′-bpy is slightly bent in order to fit into the meta-position. Meanwhile, the anchored 4,4′-bpy brings significant distortion in the regular hexagon in **1**, leading to an irregular hexagonal channel, as evidenced by the large variations in channel size parameters (Fig. S2 and S4, ESI†). The ''arrangement'' of the size-matching brace not only divides the large hexagonal channels into three small domains (one rectangle (11.13 Å × 10.98 Å) and two isosceles trapezoids (7.62 Å × 11.13 Å × 5.71 Å)), but is also expected to influence the robustness of the whole framework. PLATON calculations indicate that the effective volume of the solvent molecules is 2054.8 Å^3 per unit cell, which is 30.5% of the crystal volume.[15] The topological net of complex **2** is shown in Fig. S5 (ESI†) with the vertex symbol of $(3^6\cdot4^{13}\cdot5^9)$.

The phase purities of complexes **1** and **2** were verified by powder X-ray diffraction (PXRD) studies, which indicates that the diffraction patterns of the fresh sample are consistent with the calculated ones (Fig. S6 and S7, ESI†). Thermogravimetric analysis (TGA) was conducted on the fresh samples of **1** and **2** (Fig. S8, ESI†). A continuous weight loss of ~15% from 25 °C to 90 °C is observed on **1**, corresponding to the loss of guest solvent molecules trapped in the channels. The plot is followed by a relatively short plateau from 90 °C to 150 °C. Another continuous weight loss of ~15% from 150 °C to 300 °C indicates the removal of coordinated DMA solvent molecules. The framework of **1** starts to fall into decomposition at ~300 °C. Complex **2** exhibits a similar weight loss in the beginning. However, there is an extra plateau observed from 300 °C to 360 °C before its decomposition. Thus, this result indicates that complex **2** has a slightly higher thermal stability than complex **1**, which can be tentatively ascribed to the bridging braces of 4,4′-bpy, strengthening the framework. Moreover, the framework of **1** collapses when the solvent molecules are removed, as evidenced by PXRD patterns (Fig. S6, ESI†). In contrast, the activated sample of **2** still maintains its PXRD patterns after the solvent removal (Fig. S7, ESI†), which further underlines the enhanced robustness of complex **2**.

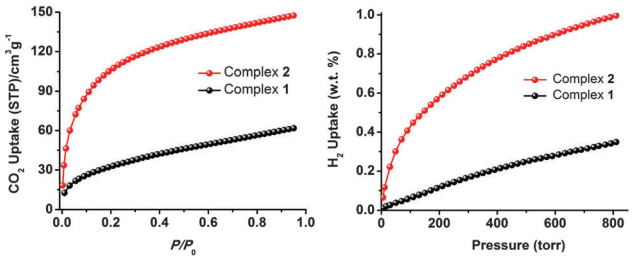

Fig. 3 (a) CO_2 adsorption isotherms of complexes **1** and **2** at 195 K and (b) H_2 adsorption isotherms of complexes **1** and **2** measured at 77 K.

To examine the permanent porosity of **1** and **2**, gas adsorption studies were performed on the activated samples. It has been observed that complex **1** does not show any adsorption toward nitrogen gas at 77 K, which is indicative of the collapse or at least partial decomposition of the structure. As shown in Fig. 3a (black dots), the CO_2 adsorption isotherm at 195 K reveals that **1** exhibits a limited uptake capacity of $\sim$61 cm^3 g^{-1} at the saturation pressure, indicating a Langmuir surface area of $\sim$148 m^2 g^{-1}. In contrast, on the basis of the CO_2 adsorption isotherm at 195 K with the capacity of $\sim$150 cm^3 g^{-1} (Fig. 3a, red dots), complex **2** possesses a much higher Langmuir surface area than complex **1**, with a value of $\sim$505 m^2 g^{-1}. Meanwhile, the activated complex **2** displays a similar behavior of no adsorption for N_2 at 77 K, which however should be presumably attributed to the relatively small pores divided by 4,4′-bpy blocking the diffusion of N_2 gas molecules. The hydrogen adsorption isotherms at 77 K show that complex **2** can adsorb a substantial of H_2 with an uptake capacity of $\sim$1.0 wt% at 1 atm of pressure, meaning an enhancement factor of 2.4 compared to complex **1** under the same conditions (Fig. 3b). Albeit complex **1** displays larger calculated accessible pore volume (52.6%) than that of complex **2** (30.5%) after the guest molecule removal, the framework of complex **2** strengthened by the ligand braces of 4,4′-bpy is able to maintain its permanent porosity.

Moreover, other gas adsorption studies were conducted on complex **2** stabilized by the ligand braces. The oxygen adsorption isotherm at 77 K shows an uptake capacity of $\sim$100 cm^3 g^{-1} at the saturation pressure (Fig. 4a). Presumably, this can be attributed to the molecular sieving effect that the segmented pores are able to discriminate between O_2 (kinetic diameter: 0.346 nm) and N_2 (kinetic diameter: 0.364 nm) molecules. As shown in Fig. 4b, complex **2** also exhibits certain

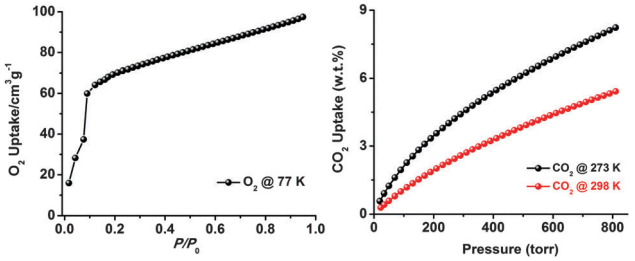

Fig. 4 (a) O_2 adsorption isotherm of complex **2** measured at 77 K and (b) CO_2 adsorption isotherms of complex **2** measured at 273 K and 298 K.

CO_2 uptake with capacities of 7.90 wt% (42 cm^3 g^{-1}) and 5.20 wt% (27 cm^3 g^{-1}) at 273 K and 298 K, respectively. The heats of adsorption (Q_{st}) of CO_2 for complex **2** were calculated using the virial method (Fig. S10, ESI†) with the initial value of $\sim$24 kJ mol^{-1} at low loadings (Fig. S11, ESI†).

In summary, the proof-of-concept work here demonstrates an effective strategy to boost the robustness of MOFs *via* introduction of size-matching ligands as braces that are deliberately anchored onto the open metal sites to support the pores. Furthermore, the inserted ligand braces segment large channels into small domains, which render a molecular sieving effect to discriminate gas molecules with different sizes. It can be envisioned that the ligand braces, coupled with extra functional sites (open metal sites for gas separation, chiral centers for asymmetric catalysis and others), can not only enhance the framework robustness, but also facilitate task-specific applications, which creates an interesting scenario in the MOF field.

The support from the National Natural Science Foundation of China (No. 21171025 and 21471021), and the Program of Innovative Research Team in University of Liaoning Province (LT2012020) is gratefully acknowledged. S. Ma acknowledges NSF (DMR-1352065) and USF for financial support of this work.

Notes and references

§ X-Ray crystal data for complex **1**: $C_{64}H_{24}Co_3N_5O_{18.75}$, f_w = 1339.75, trigonal, $P\bar{3}_1c$, a = 15.3816(3), b = 15.3816(3), c = 16.8215(4) Å, V = 3446.66(16) Å^3, Z = 2, T = 233(2) K, ρ_{calcd} = 1.291 g cm^{-3}, R_1 ($I > 2\sigma(I)$) = 0.0571, wR_2 (all data) = 0.1671, CCDC 1436005. X-Ray crystal data for complex **2**: $C_{69}H_{32}Co_3N_{5.75}O_{15}$, f_w = 1358.29, monoclinic, $P2_1/n$, a = 15.6069(4), b = 26.4325(8), c = 16.6221(5) Å, V = 6857.1(3) Å^3, Z = 4, T = 233(2) K, ρ_{calcd} = 1.316 g cm^{-3}, R_1 ($I > 2\sigma(I)$) = 0.0695, wR_2 (all data) = 0.2069, CCDC 1435998.

1 (*a*) H.-C. Zhou and S. Kitagawa, *Chem. Soc. Rev.*, 2014, **43**, 5415; (*b*) H. Furukawa, K. E. Cordova, M. O'Keeffe and O. M. Yaghi, *Science*, 2013, **341**, 1230444.
2 (*a*) M. O'Keeffe and O. M. Yaghi, *Chem. Rev.*, 2012, **112**, 675; (*b*) W. Lu, Z. Wei, Z.-Y. Gu, T.-F. Liu, J. Park, J. Park, J. Tian, M. Zhang, Q. Zhang, T. Gentle III, M. Bosch and H.-C. Zhou, *Chem. Soc. Rev.*, 2014, **43**, 5561; (*c*) W.-Y. Gao and S. Ma, *Comments Inorg. Chem.*, 2014, **34**, 125.
3 (*a*) Y. He, W. Zhou, G. Qian and B. Chen, *Chem. Soc. Rev.*, 2014, **43**, 5657; (*b*) K. Sumida, D. L. Rogow, J. A. Mason, T. M. McDonald, E. D. Bloch, Z. R. Herm, T.-H. Bae and J. R. Long, *Chem. Rev.*, 2012, **112**, 724; (*c*) E. Barea, C. Montoro and J. A. R. Navarro, *Chem. Soc. Rev.*, 2014, **43**, 5419; (*d*) P. Nugent, Y. Belmabkhout, S. D. Burd, A. J. Cairns, K. Forrest, S. Ma, B. Space, L. Wojtas, R. Luebke, M. Eddaoudi and M. J. Zaworotko, *Nature*, 2013, **495**, 80.
4 (*a*) M. Yoon, R. Srirambalaji and K. Kim, *Chem. Rev.*, 2012, **112**, 1196; (*b*) A. Dhakshinamoorthy and H. Garcia, *Chem. Soc. Rev.*, 2014, **43**, 5750; (*c*) J. Liu, L. Chen, H. Cui, J. Zhang, L. Zhang and C.-Y. Su, *Chem. Soc. Rev.*, 2014, **43**, 6011; (*d*) T. Zhang and W. Lin, *Chem. Soc. Rev.*, 2014, **43**, 5982.
5 (*a*) L. E. Kreno, K. Leong, O. K. Farha, M. Allendorf, R. P. Van Duyne and J. T. Hupp, *Chem. Rev.*, 2012, **112**, 1105; (*b*) Z. Hu, B. J. Deibert and J. Li, *Chem. Soc. Rev.*, 2014, **43**, 5815.
6 (*a*) W.-Y. Gao, M. Chrzanowski and S. Ma, *Chem. Soc. Rev.*, 2014, **43**, 5841; (*b*) V. Stavila, A. A. Talin and M. D. Allendorf, *Chem. Soc. Rev.*, 2014, **43**, 5994; (*c*) P. Ramaswamy, N. E. Wong and G. K. H. Shimizu, *Chem. Soc. Rev.*, 2014, **43**, 5913; (*d*) J.-P. Zhang, P.-Q. Liao, H.-L. Zhou, R.-B. Lin and X.-M. Chen, *Chem. Soc. Rev.*, 2014, **43**, 5789; (*e*) M. Eddaoudi, D. F. Sava, J. F. Eubank, K. Adil and V. Guillerm, *Chem. Soc. Rev.*, 2015, **44**, 228.
7 P. Horcajada, R. Gref, T. Baati, P. K. Allan, G. Maurin, P. Couvreur, G. Férey, R. E. Morris and C. Serre, *Chem. Rev.*, 2012, **112**, 1232.

8 (*a*) N. C. Burtch, H. Jasuja and K. S. Walton, *Chem. Rev.*, 2014, **114**, 10575; (*b*) O. K. Farha and J. T. Hupp, *Acc. Chem. Res.*, 2010, **43**, 1166.
9 (*a*) G. Férey, C. Mellot-Draznieks, C. Serre, F. Millange, J. Dutour, S. Surblé and I. Margiolaki, *Science*, 2005, **309**, 2040; (*b*) J. H. Cavka, S. Jakobsen, U. Olsbye, N. Guillou, C. Lamberti, S. Bordiga and K. P. Lillerud, *J. Am. Chem. Soc.*, 2008, **130**, 13850; (*c*) H. Furukawa, F. Gandara, Y.-B. Zhang, J. Jiang, W. L. Queen, M. R. Hudson and O. M. Yaghi, *J. Am. Chem. Soc.*, 2014, **136**, 4369; (*d*) Y. Chen, T. Hoang and S. Ma, *Inorg. Chem.*, 2012, **51**, 12600; (*e*) H.-L. Jiang, D. Feng, K. Wang, Z.-Y. Gu, Z. Wei, Y.-P. Chen and H.-C. Zhou, *J. Am. Chem. Soc.*, 2013, **135**, 13934; (*f*) W.-Y. Gao, R. Cai, L. Meng, L. Wojtas, W. Zhou, T. Yildirim, X. Shi and S. Ma, *Chem. Commun.*, 2013, **49**, 10516; (*g*) W.-Y. Gao, W. Yan, R. Cai, L. Meng, A. Salas, X.-S. Wang, L. Wojtas, X. Shi and S. Ma, *Inorg. Chem.*, 2012, **51**, 4423.
10 (*a*) S. R. Batten and R. Robson, *Angew. Chem., Int. Ed.*, 1998, **37**, 1460; (*b*) J. L. C. Rowsell and O. M. Yaghi, *J. Am. Chem. Soc.*, 2006, **128**, 1304; (*c*) S. Ma, X.-S. Wang, D. Yuan and H.-C. Zhou, *Angew. Chem., Int. Ed.*, 2008, **48**, 4130; (*d*) S. Ma, D. Sun, M. Ambrogio, J. A. Fillinger, S. Parkin and H.-C. Zhou, *J. Am. Chem. Soc.*, 2007, **129**, 1858; (*e*) W.-Y. Gao, Z. Zhang, L. Cash, L. Wojtas, Y.-S. Chen and S. Ma, *CrystEngComm*, 2013, **15**, 9320.
11 (*a*) W.-Y. Gao, R. Cai, T. Pham, K. A. Forrest, A. Hogan, P. Nugent, K. Williams, L. Wojtas, R. Luebke, L. J. Weselinski, M. J. Zaworotko, B. Space, Y.-S. Chen, M. Eddaoudi, X. Shi and S. Ma, *Chem. Mater.*, 2015, **27**, 2144; (*b*) V. Colombo, S. Galli, H. J. Choi, G. D. Han, A. Maspero, G. Palmisano, N. Masciocchi and J. R. Long, *Chem. Sci.*, 2011, **2**, 1311; (*c*) H. Jasuja, Y. Jiao, N. C. Burtch, Y.-g. Huang and K. S. Walton, *Langmuir*, 2014, **30**, 14300; (*d*) J.-P. Zhang, Y.-B. Zhang, J.-B. Lin and X.-M. Chen, *Chem. Rev.*, 2012, **112**, 1001.
12 (*a*) W. Zhang, Y. Hu, J. Ge, H.-L. Jiang and S.-H. Yu, *J. Am. Chem. Soc.*, 2014, **136**, 16978; (*b*) Z. Wang and S. M. Cohen, *Chem. Soc. Rev.*, 2009, **38**, 1315; (*c*) J. B. Decoste, G. W. Peterson, M. W. Smith, C. A. Stone and C. R. Willis, *J. Am. Chem. Soc.*, 2012, **134**, 1486; (*d*) K. P. Rao, M. Higuchi, K. Sumida, S. Furukawa, J. Duan and S. Kitagawa, *Angew. Chem., Int. Ed.*, 2014, **53**, 8225.
13 (*a*) Y.-X. Tan, Y.-P. He and J. Zhang, *Inorg. Chem.*, 2012, **51**, 9649; (*b*) D. Tian, Q. Chen, Y. Li, Y.-H. Zhang, Z. Chang and X.-H. Bu, *Angew. Chem., Int. Ed.*, 2014, **53**, 837; (*c*) X. Zhao, X. Bu, Q.-G. Zhai, H. Tran and P. Feng, *J. Am. Chem. Soc.*, 2015, **137**, 1396; (*d*) H. Wang, J. Xu, D.-S. Zhang, Q. Chen, R.-M. Wen, Z. Chang and X.-H. Bu, *Angew. Chem., Int. Ed.*, 2015, **54**, 5966.
14 (*a*) S. Ma, J. M. Simmons, D. Yuan, J.-R. Li, W. Weng, D.-J. Liu and H. C. Zhou, *Chem. Commun.*, 2009, 4049; (*b*) Q. Gao, Y.-B. Xie, J.-R. Li, D.-Q. Yuan, A. A. Yakovenko, J.-H. Sun and H.-C. Zhou, *Cryst. Growth Des.*, 2012, **12**, 281.
15 A. L. Spek, *PLATON, A Multipurpose Crystallographic Tool*, Utrecht University, Utrecht, The Netherlands, 2001.

